Aged but withstanding: maintenance of growth rates in old pines is not related to enhanced water-use efficiency

Elena Granda[1*], J. Julio Camarero[1], J. Diego Galván[2], Gabriel Sangüesa-Barreda[1], Arben Q. Alla[3], Emilia Gutierrez[4], Isabel Dorado-Liñán[5], Laia Andreu-Hayles[6], Inga Labuhn[7], Håkan Grudd[8] and Jordi Voltas[9]

[1]Instituto Pirenaico de Ecología (IPE-CSIC), Avda. Montañana 1005, E-50192 Zaragoza, Spain; jjcamarero@ipe.csic.es; gsanguesa@ipe.csic.es

[2]Swiss Federal Research Institute WSL, Zuercherstrasse 111, 8903 Birmensdorf, Switzerland; galiarde@gmail.com

[3]Fakulteti i Shkencave Pyjore, Universiteti Bujqësor i Tiranës, Kodër-Kamëz 1029, Tirana, Albania; benialla@gmail.com

[4]Departament de Biologia Evolutiva, Ecologia i Ciències Ambientals, Facultat de Biologia, Universitat de Barcelona, Avd. Diagonal 643, 08028 Barcelona, Spain; emgutierrez@ub.edu

[5]Forest Research Centre, Instituto Nacional de Investigación y Tecnología Agraria y Alimentaria (INIA-CIFOR), Madrid, Spain; dorado.isabel@inia.es

[6]Tree-Ring Laboratory, Lamont-Doherty Earth Observatory of Columbia University, 61 Route 9W, Palisades, NY 10964, USA; lah@ldeo.columbia.edu

[7]Department of Physical Geography and Quaternary Geology, Stockholm University, Sweden; present address at Department of Geology, Lund University, Sweden; inga.labuhn@geol.lu.se

[8]Department of Physical Geography and Quaternary Geology, Bolin Centre for Climate Research, Stockholm University, Sweden; hakan.grudd@polar.se

[9]Department of Crop and Forest Sciences-AGROTECNIO Center, Universitat de Lleida, Rovira Roure 191, E 25198 Lleida, Spain; jvoltas@pvcf.udl.cat

*Corresponding author:

Elena Granda

Instituto Pirenaico de Ecología (IPE-CSIC)

Avda. Montañana 1005, 50192 Zaragoza, Spain.

Phone: +34 976 369393 ext. 880039/ Fax: +34 976 716019

E-mail address: elena.granda.f@gmail.com

Abstract

Growth of old trees in cold-limited forests may benefit from recent climate warming and rising atmospheric CO_2 concentrations (c_a) if age-related constraints do not impair wood formation. To test this hypothesis, we studied old Mountain pine trees at three Pyrenean high-elevation forests subjected to cold-wet (ORD, AIG) or warmer-drier (PED) conditions. We analyzed long-term trends (1450-2008) in growth (BAI, basal area increment), maximum (MXD) and minimum (MID) wood density, and tree-ring carbon ($\delta^{13}C$) and oxygen ($\delta^{18}O$) isotope composition, which were used as proxies for intrinsic water-use efficiency (iWUE) and stomatal conductance (g_s), respectively. Old pines showed positive (AIG and ORD) or stable (PED) growth trends during the industrial period (since 1850) despite being older than 400 years. Growth and wood density covaried from 1850 onwards. In the cold-wet sites (AIG and ORD) enhanced photosynthesis through rising c_a was likely responsible for the post-1850 iWUE improvement. However, uncoupling between BAI and iWUE indicated that increases in iWUE were not responsible for the higher growth but climate warming. A reduction in g_s was inferred from increased $\delta^{18}O$ for PED trees from 1960 onwards, the warmest site where the highest iWUE increase occurred (34%). This suggests that an emergent drought stress at warm-dry sites could trigger stomatal closure to avoid excessive transpiration. Overall, carbon acquisition as lasting woody pools is expected to be maintained in aged trees from cold and high-elevation sites where old forests constitute unique long-term carbon reservoirs.

*Keywords***:** cold-limited forests; dendroecology; global change; old trees; *Pinus uncinata*; stable isotopes

Abbreviations: basal area increment (BAI); maximum wood density (MXD); minimum wood density (MID); intrinsic water use efficiency (iWUE), photosynthetic rates (A), and stomatal conductance (g_s).

1. Introduction

Old-growth forests represent 15% of the world forest surface and are responsible for 10% of the global net ecosystem productivity (Luyssaert et al. 2008) given that they have been taking up carbon for centuries and storing it as long-lasting woody pools. In fact, tree longevity rather than growth rates is considered to control the carbon sequestration of forests (Körner, 2017).

A progressive reduction in the productivity of old forests is traditionally assumed because aged trees are thought to show a decline in growth and carbon accumulation due to a less efficient hydraulic architecture, cell senescence, and a decreased nutrient uptake (Yoder et al. 1994; Ryan & Yoder 1997; Mencuccini 2002) or an increase of maintenance respiration costs (Yoda et al. 1965). However, recent studies have shown that carbon accumulation may continue until trees are centuries old (Stephenson et al. 2014) since tree size, rather than age, drives long-term growth trends (Mencuccini et al. 2005). Yet, there is an important need to understand old trees' performance, especially in regard to their responses to rapidly changing environmental conditions (climate warming, rising atmospheric CO_2 concentrations –c_a).

During the industrial period (here defined from 1850 onwards) environmental changes have been more pronounced and rapid, including abrupt rises in c_a and air temperatures (IPCC 2014). Increases in c_a could lead to the so-called fertilization effect, which predicts a positive influence of greater carbon availability on tree growth through enhanced net photosynthetic rates (Huang et al. 2007; Streit et al. 2014, but see Körner 2003). On the other hand, rising temperatures could also stimulate photosynthesis, growth, and thus productivity, in cold-limited sites such as high-elevation forests (Gunderson et al. 2009; Salzer et al. 2009; Way & Oren 2010) although carbon acquisition (photosynthesis) is less limited by low temperatures than carbon use in

88 tissue formation (Körner 2015). Several studies have addressed tree responses to higher
89 c_a and warming through the inference of long-term changes in intrinsic water-use
90 efficiency (or carbon gain per unit of water lost, hereafter iWUE) and its relationship
91 with growth, reporting contrasting or a lack of relationships between them (Saurer et al.
92 2004; Silva et al. 2009; Andreu-Hayles et al. 2011; Peñuelas et al. 2011; Silva &
93 Horwath 2013; Fardusi et al. 2016). Interestingly, tree age has been found to be a
94 relevant factor acting on the rate of growth change as c_a rises. For instance, Voelker et
95 al. (2006) reported an ontogenetic decline in the rate of c_a growth stimulation in
96 *Quercus* and *Pinus* species, and Camarero et al. (2015a) found that the largest growth
97 improvements of mountain pines occurred in young trees. However, less is known about
98 old-trees, making them interesting subjects to evaluate long-term functional responses
99 to rapid environmental changes.

100 Indeed, whether old-forest productivity is enhanced or not under future
101 environmental conditions may strongly influence terrestrial carbon cycles (Babst et al.
102 2014a). The role played by forests as carbon sinks warrants accurate investigation of
103 both radial growth and wood density to improve the estimations of carbon uptake as
104 woody biomass (Bouriaud et al. 2015). Wood density is related to carbon fixation and
105 water economy (Babst et al. 2014b), but its relationship with iWUE has rarely been
106 addressed despite being a key trait linking hydraulic conductivity, growth, carbon use to
107 synthesize wood and mechanical strength (but see Ponton et al. 2001; Olano et al. 2014;
108 Pellizzari et al. 2016 for studies relating C isotopes with wood anatomy). In conifers, a
109 less dense earlywood (often represented by a lower ring minimum density, MID)
110 usually translates into wider conduit lumen areas, which provides higher hydraulic
111 conductivity (Camarero et al. 2014). Conversely, a denser latewood (represented by
112 higher maximum density, MXD) is linked to a higher carbon investment in thickening

and lignification of cell walls (Hacke et al. 2001). Therefore, the specific tree processes contributing to changes in growth and wood density have to be investigated to understand responses to current environmental changes, the associated carbon allocation trade-offs and the mechanisms involved.

Old trees may modify their water and carbon economies in response to environmental changes. In the long-term, these changes can be estimated using stable isotopes in tree rings (Farquhar et al. 1982; McCarroll & Loader 2004). For instance, the relative importance of changes in stomatal conductance (g_s) and photosynthetic rate (A) affecting tree performance can be determined by the simultaneous study of carbon ($\delta^{13}C$) and oxygen ($\delta^{18}O$) isotope composition (e.g. Nock et al. 2010). While many studies have reported current increasing trends in iWUE (Saurer et al. 2014) it is not always obvious whether they are the result of photosynthetic stimulation (A increase), stomatal regulation (g_s decrease) or a combination of both (e.g. Streit et al. 2014). Considering that ^{18}O enrichment in tree-ring wood may be influenced by a reduction in relative humidity (as related to lower *gs*; Saurer et al.1997; Treydte et al. 2014) but not by changes in A, the combined study of $\delta^{13}C$ and $\delta^{18}O$ allows elucidating whether biochemical or stomatal controls of photosynthesis underlie changes in iWUE (Scheidegger et al. 2000; Barbour et al. 2002; Grams et al. 2007).

High-elevation forests dominated by tree species such as Mountain pine (*Pinus uncinata*) are expected to be especially sensitive to ongoing changes in environmental conditions (Körner 2012). In the case of the Pyrenees, radial growth of Mountain pine is limited by low temperatures during the growing season and the previous fall (Tardif et al. 2003). Additionally, Mountain pine trees from wet sites exhibit growth enhancement concurrent with the c_a rise, which is consistent with a fertilization effect only on those particularly wet habitats (Camarero et al. 2015b). Therefore, we hypothesize that

138 temperature and c_a increases might benefit these old forests through mechanisms such
139 as an increase in C sink activities, an extended growing season, higher carbon inputs or
140 a combination of them. However, drought stress due to higher evapotranspiration could
141 be an emergent limiting factor by reducing stomatal conductance and photosynthetic
142 rates in Mountain pine forests, especially in sites located on rocky substrates and steep
143 slopes or experiencing higher warming rates (Galván et al. 2015; Churakova (Sidorova)
144 et al. 2016).

145 The aim of our study is to determine if the performance of old Mountain pines
146 (comprising ages from 412 to 731 years) inhabiting cold-limited and high-elevation
147 sites has been modified by the industrial rise in c_a and temperatures. To this end, we
148 quantify long-term changes in radial growth, wood density, $\delta^{13}C$ and $\delta^{18}O$ by comparing
149 several Pyrenean forests with similarly aged trees but different local conditions.
150 Particularly, we pose the following questions to understand possible trade-offs of carbon
151 allocation to secondary growth: i) which are the main differences in growth, wood
152 density and physiological adjustments of old pines from high-elevation forests with
153 distinct temperatures and humidity conditions between pre- (1700-1849) and industrial
154 (1850-2008) periods?; ii) are these old pines experiencing growth enhancement in
155 response to warmer conditions and/or higher c_a?; iii) are shifts in iWUE the result of
156 changes in the tree's photosynthetic capacity (A) or stomatal conductance (g_s) and iv)
157 which are the relationships among growth, wood density (MID, MXD), $\delta^{18}O$ and iWUE
158 and do they change through time? We hypothesize that higher c_a and current warmer
159 temperatures may sustain or even enhance old trees' growth. Based on the conceptual
160 framework outlined in Figure 1, we test the following hypotheses: (i) improved iWUE
161 may be positively linked to enhanced growth and increased MXD since the industrial
162 period; (ii) MID and MXD are positively correlated if both variables are limited by low

temperatures which drive cambium activity, although a negative correlation could be expected if lower lumen area of earlywood tracheids (higher MID) limits the carbon acquisition for MXD; (iii) a greater growth is expected under higher hydraulic conductivity due to a higher efficiency (larger conduit area and thus, lower MID) under a warmer climate; and (iv) higher MID (lower potential hydraulic conductivity) would be related to increased iWUE if a reduction in hydraulic conductivity is linked to decreased g_s.

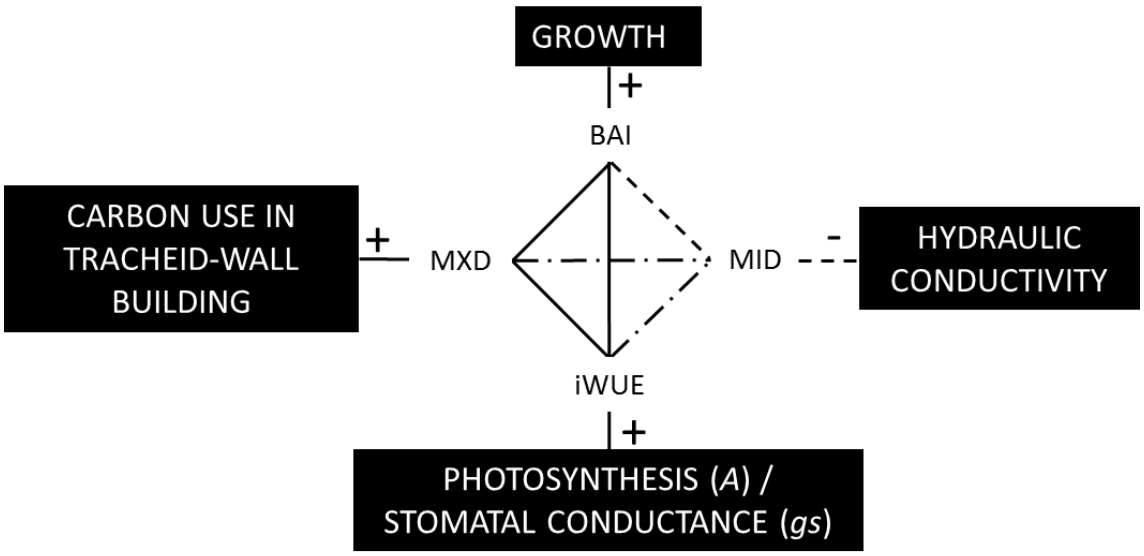

Figure 1. Conceptual model describing the main hypothesis regarding BAI, MXD, MID and iWUE (and their interpretation in the black boxes) regarding long-term changes in performance of old trees from cold-limited forests under warmer temperatures and increasing c_a. Solid and broken lines represent expected positive and negative relationships, respectively. The relationships between MXD and MID, and between iWUE and MID are conditional (represented as dashed-dotted lines), as explained at the end of the introduction section (1). Variables' abbreviations are: basal area increment (BAI); maximum wood density (MXD); minimum wood density (MID); intrinsic water use efficiency (iWUE), photosynthetic rates (A), and stomatal conductance (g_s).

2. Materials and Methods

2.1. Sampling species and sites

The study species is Mountain pine (*Pinus uncinata* Ram.), which dominates high-elevation forests in the Spanish Pyrenees, where it forms most forest limits and treelines (Camarero & Gutiérrez 1999). Mountain pine is a shade-intolerant, slow-growing conifer, which may reach 800-1000 years in age (Camarero & Gutiérrez 1999). Radial growth of Mountain pine peaks in July whilst latewood formation starts in August or September, and the growing period encompasses from May to October (Camarero et al. 1998).

The sampling sites are located in protected areas of the Spanish Pyrenees (Table 1): "Ordesa y Monte Perdido" National Park (hereafter ORD: 2,088 m a.s.l; 42º 40' N, 00º 03' E); "Aigüestortes i Estany de Sant Maurici" National Park (hereafter AIG: 2,355 m a.s.l.; 42º 35' N, 00º 57' E); and Pedraforca Regional Park located in the "Cadí-Moixeró" Natural Park (hereafter PED: 2,100 m a.s.l.; 42º 14' N, 01º 42' E). These protected areas guarantee the preservation of old stands, which can be considered free of local anthropogenic disturbances (e.g., logging, fires). Pyrenean forests situated near the forest limit and the treeline usually form low-density, open-canopy stands that are located in steep and elevated sites over rocky substrates with thin soils forming isolated patches (Galván et al. 2014). Soils in ORD and PED are mainly basic and developed on calcareous substrates, whereas soils in AIG are acid (umbric leptosols) formed on granodiorites.

The three Pyrenean high-elevation forests are located just below the forest limit and exposed to cold and relatively wet climate conditions. Nonetheless, climate is distinct among the three areas (Table 1), allowing for comparison of old-tree responses under varying conditions. ORD is the lowest altitude site and AIG is the most elevated

206 one (Tables 1 and S1). PED is the easternmost, warmest and driest site despite receiving
207 high rainfall in summer and autumn, i.e. in the late growing season, due to its proximity
208 to the Mediterranean Sea. Contrastingly, ORD is the westernmost and wettest site and
209 receives the highest precipitation in winter and spring, i.e. in the early growing season,
210 due to a marked influence of Atlantic fronts. AIG represents the coldest and most
211 continental site, with a mean annual temperature of 3.1 ºC (Table 1). From 1950 to 2009
212 mean temperatures (CRU TS 3.1 dataset; 1901–2002, Harris et al. 2014) increased at
213 rates of +0.3º, +0.3º and +0.2 ºC per decade during the growing season (May-October)
214 in ORD, AIG and PED, respectively. The warming rates were more pronounced during
215 the last decades, particularly since the 1980s, but no changes were observed in
216 precipitation regime. Warming rates of +2.8º to 4 °C are forecasted for the 21st century
217 in the Spanish Pyrenees (López-Moreno et al. 2008).

Table 1. Description of the study sites and weather stations used to characterize the climatic gradient. The trends refer to the mean annual temperature (T) and total annual precipitation (P) during the growing season (May to October) calculated using the CRU 0.5º-gridded climate dataset (Harris et al., 2014) for the period 1950-2008 (** p-value < 0.05; *** p-value < 0.001 and ns represents non-significant results). Rain $\delta^{18}O$ was estimated according to Ferrio and Voltas (2005).

						Local climate data			CRU climate data			
Study site	**Coordinates**	**Aspect**	**Slope**	**Bedrock/soil type**	**Altitude of trees (m a.s.l.)**	**Station (elevation in m, distance to sampled sites)**	**Period of local climate data**	**Mean annual T (ºC)**	**Total annual P (mm)**	**Trend T (ºC yr^{-1})**	**Trend P (mm yr^{-1})**	**Rain $\delta^{18}O$ (‰)**
ORD	42º 39' 52" N 0º 00' 59" E	N	49º	Calcareous limestones, marls/ Entisol	2120 ± 89	Refugio de Góriz (2200 m, 8 km)	1982-2013	4.8	1718	0.03***	-0.63 ns	-7.99
AIG	42º 38' 49" N 0º 50' 05" E	SE	35º	Siliceous granodiorite/ umbric leptosols	2293 ± 42	Port de la Bonaigua (2266 m, 5 km)	1998-2014	3.1	1221	0.03***	-0.68 ns	-8.35
PED	42º 20' 57" N 1º 57' 22" E	NE	36º	Calcareous limestones, marls/ entisol	2205 ± 16	La Molina (1711 m, 21 km)	1955-1969	5.6	1209	0.019**	-1.1 ns	-8.77

222 *2.2. Dendroecological methods*

223 A total of 10, 37 and 22 old trees (ages over 400 years) were sampled between 2008 and
224 2009 in ORD, AIG and PED sites, respectively, of which 10, 17 and 11 were also used
225 for wood density measurements. Among them, four trees per site (those with the longest
226 time spans, 412-731 years old; see Table S1 for details) were selected for $\delta^{13}C$ and $\delta^{18}O$
227 analyses.

228 Topographic (altitude, slope, aspect; see Table 1) and biometric variables (DBH:
229 diameter at breast height –measured at 1.3 m-; tree height) were recorded for each tree
230 (see Table S1 in Supporting Information). All individuals were cored at 1.3 m using 5-,
231 10- and 12-mm Pressler increment borers taking at least five cores per tree. The mean
232 DBH (±SD) was 66.4 ± 12.4 cm, 59.0 ± 7.4 cm and 58.7 ± 3 cm in ORD, AIG and PED
233 respectively. Mean ages were 486 ± 31 years, 557 ± 22 years and 528 ± 40 years for
234 ORD, AIG and PED, respectively.

235 Two cores per tree were mounted and sanded with sandpapers of progressively
236 fine grain until tree rings were clearly visible to obtain growth data (Stokes & Smiley
237 1968). Then, the samples were visually cross-dated and measured to a precision of 0.01
238 mm using a LINTAB measuring device (Rinntech, Heidelberg, Germany). Cross-dating
239 and ring width measurements were evaluated using COFECHA, which calculates cross
240 correlations between individual series of each core and a master chronology, obtained
241 averaging all measured series in each site (Holmes 1983).

242 Ring-width series were converted to basal area increment (BAI) assuming
243 concentric circularity. BAI removes variation in growth attributable to increasing stem
244 circumference and captures changes in growth better than linear measures such as tree-
245 ring width (Biondi & Qeadan 2008). The annual BAI was calculated as follows:

246 $$BAI = \pi (r_t^2 - r_{t-1}^2) \quad (1)$$

where r_t and r_{t-1} are the stem radii in the current (t) and previous (t-1) years. In the case of cores without pith, we estimated the length of the missing part of the radius by fitting a geometric pith locator to the innermost rings (Duncan 1989).

2.3. Wood density

The trees selected for density and isotope analyses corresponded to the oldest trees with the highest correlation with tree-ring width site chronology (see Table S2 in Supporting Information). Two cores (10-12-mm) from each selected tree were used for density measurements. These cores were glued onto wooden supports and thin wooden laths (1 mm) were cut out with a twin-bladed saw. Density was measured with an Itrax Wood Scanner from Cox Analytical Systems (http://www.coxsys.se) at the Dendrolab of the University of Stockholm (Sweden), where laths are scanned using a focused high-energy X-ray beam. The radiographic images were analysed with the software WinDendro (Regent Instruments, Canada), which performs a light calibration of the grey values using a calibration wedge (Grudd 2008).

2.4. Wood carbon and oxygen isotopes: tree-ring selection and cellulose extraction

The best four cross-dating old trees per site were used in order to maximize the isotopic signal common to the sampled trees while keeping the workload of sample processing under reasonable limits. Whole non-sanded tree rings were separated manually from one core of each selected tree for the period 1850-2008, and pools of 10 rings corresponding to each decade were considered for the 1450s-1840s period in ORD and AIG sites. In PED, two years per decade (corresponding to the initial and the central year) were measured for the period of 1450-1890, and both years were averaged for each decade for statistical analyses. We analysed the entire tree rings because the narrow width of

the rings in these old trees did not provide sufficient material for analysing earlywood and latewood separately. We extracted cellulose from 2 mg of wood per individual sample. Cellulose extraction was performed to obtain purified α-cellulose based on a modification of the method of Leavitt & Danzer (1993) for the removal of extractives and lignin, as detailed in Ferrio & Voltas (2005).

2.5. Carbon and oxygen isotopes

For $\delta^{13}C$, dry α-cellulose was weighed (0.30–0.40 mg) into tin foil capsules and combusted using a Flash EA-1112 elemental analyser interfaced with a Finnigan MAT Delta C isotope ratio mass spectrometer (Thermo Fisher Scientific Inc.). For $\delta^{18}O$, 0.30–0.40 mg of dry α-cellulose was weighed into silver foil capsules and combusted using a Carlo Erba 1108 elemental analyser (Carlo Erba Instruments Ltd., Milan, Italy) interfaced with a Finnigan Deltaplus XP isotope ratio mass spectrometer (Thermo Fisher Scientific Inc.). Isotope ratios were expressed as per mil deviations using the δ notation relative to Vienna Pee Dee Belemnite (VPDB) standard (for carbon) and Vienna Standard Mean Ocean Water (VSMOW) standard (for oxygen):

$$\delta^{n}X\ (‰) = [(R_{sample}/R_{standard}) - 1] \times 1000 \quad (2)$$

where $\delta^{n}X$ stands for the isotopic composition, in parts per mil (‰) of the heavier isotope, and R_{sample} and $R_{standard}$ represent the $^{13}C/^{12}C$ or $^{18}O/^{16}O$ ratios of the sample and the VPDB or VSMOW international standards, respectively (Farquhar, Oleary & Berry 1982). The accuracy of the analyses (SD of working standards) was 0.06‰ ($\delta^{13}C$) and 0.25‰ ($\delta^{18}O$).

To account for changes in the $\delta^{13}C$ of atmospheric CO_2 ($\delta^{13}c_a$), we calculated carbon isotope discrimination in cellulose ($\Delta^{13}C$) from $\delta^{13}c_a$ and plant $\delta^{13}C$ ($\delta^{13}c_p$), as described by Farquhar & Richards (1984):

297 $$\Delta^{13}C = (\delta^{13}c_a - \delta^{13}c_p)/(1+\delta^{13}c_p/1000) \quad (3)$$

298

299 *2.6. Intrinsic water-use efficiency*

300 Following Farquhar et al. (1982) we estimated intrinsic water-use efficiency (iWUE)
301 using the equation:

302 $$\text{iWUE} = A/g_s = c_a\,[1-(\,c_i / c_a\,)]\,0.625, \quad (4)$$

303 where A is the rate of net photosynthesis, g_s is stomatal conductance to H_2O, c_i is
304 intercellular CO_2 concentration, c_a is the ambient air CO_2 concentration, and 0.625 is the
305 relative diffusivity of CO_2 compared to that of water vapour due to the higher molecular
306 weight of the former (0.625 $g_{H2O} = g_{CO2}$). To determine c_i we used the following
307 equation proposed by Francey & Farquhar (1982):

308 $$c_i = [(\Delta^{13}C - a) \times c_a] / (b - a), \quad (5)$$

309 where $\Delta^{13}C$ is the isotope discrimination (see eq. 3), a is the diffusion fractionation
310 across the boundary layer and the stomata (4.4‰), and b is the Rubisco enzymatic
311 biologic fractionation (27.0‰). The long-term c_a and atmospheric $\delta^{13}C$ data from 1971
312 to 1994 were obtained from McCarroll & Loader (2004). Additional data for c_a and
313 $\delta^{13}c_a$ were taken from the Earth System Research Laboratory web site
314 (http://www.esrl.noaa.gov/gmd/about/aboutgmd.htm; see Fig. S1 for c_a). Lastly, three
315 theoretical scenarios for changes in iWUE as a function of changes in c_a *and* c_i (constant
316 c_i, constant c_i/c_a and constant c_a-c_i) were calculated following (Saurer et al. 2004).

317

318 *2. 7. Climate data*

319 To estimate past annual temperature variability (Fig. S1) we used two climate
320 reconstructions based on tree-ring density (Dorado Liñán et al. 2012); 1450-2008
321 period) and on historical temperature records (Agustí-Panareda et al. 2000; 1781-1997

period). These records were normalized and plotted as temperature anomalies (Fig. S1). Recent (1950-2008 period) mean monthly temperature and total monthly precipitation were obtained for each site from the CRU TS3.1 gridded 0.5º resolution dataset product (Harris et al. 2014), and used for correlation analyses involving tree variables (BAI, MXD, MID, $\delta^{18}O$ and iWUE).

2.8. Data analyses

Differences among sites and through time were conducted using analyses of covariance (ANCOVA) for each response tree variable (BAI, MXD, MID, $\delta^{18}O$ and iWUE), with site as fixed factor and year as a covariate. The pre- (from 1700 to 1849, decadal values) and industrial periods (from 1850 to 2008, annual values) were analyzed separately. The covariance structure was modeled as first-order autoregressive (i.e., AR[1]) to account for correlated errors in the case of yearly data. Temporal trends were also estimated separately for each site and pairwise comparisons among the three sites were performed using Tukey HSD tests. For each tree variable we assessed significant differences between the two periods through Student *t* tests. Pearson correlation coefficients were computed to assess the relationships between tree and seasonal climatic variables. Moving correlations of 40 years lagged by one year were also computed among iWUE and $\delta^{18}O$ to check for changes in the association between these two variables.

The predictive ability of the three iWUE scenarios was evaluated using the Root Mean Square Predictive Difference (RMSPD, Choury et al. 2017). The RMSPD is the root square of the sum of absolute differences between actual and predicted values divided by the number of observations. All statistical analyses were conducted using the R language version 3.1.1. (R Development Core Team, 2014).

3. Results

3.1. Long-term trends in growth and wood density

During the pre-industrial period we found slightly decreasing BAI trends over time, in contrast with the positive BAI trends found during the industrial period (Table 2, Fig. 2). However, we observed that such increases were highest at AIG followed by ORD, while BAI values at PED were sustained during this industrial period (Table 3). BAI and MXD clearly dropped during cold periods (Fig. S1), particularly in the early 18th (1700s) and 19th centuries (1810-1830) or during the 1970s (Figs. 2, 3). We observed overall declining MXD values but stable MID values in the pre-industrial period, although significant differences were found among sites (Table 2). Considering the industrial period, declining trends were found for MXD and MID, with the exception of MXD in PED (Tables 2, 3; Fig. 3).

Table 2. Significant differences across time, among sites (ORD, AIG, PED) and their interaction for each study trait and two different periods corresponding to pre- (1700-1849, decadal values) and industrial (1850-2008, annual values) periods. Variables' abbreviations are: basal area increment (BAI); maximum wood density (MXD); minimum wood density (MID); oxygen isotopic composition ($\delta^{18}O$) and intrinsic water use efficiency (iWUE). Site differences are also provided, where symbols ">" and "=" indicate a significant higher value and a non-significant difference between sites, respectively.

		Pre-industrial period (1700-1849)			Industrial period (1850-2008)		
		F	*P* value	Site differences	*F*	*P* value	Site differences
BAI	Site	38.54	<0.0001	PED > ORD > AIG	203.63	<0.0001	PED > ORD = AIG
	Time	5.6	0.02		9.58	0.002	
	Site* Time	3.67	0.03		4.61	0.01	
MXD	Site	403.73	<0.0001	PED > ORD > AIG	855.66	<0.0001	PED > ORD > AIG
	Time	21.24	<0.0001		55.26	<0.0001	
	Site* Time	9.29	0.0005		13.04	<0.0001	
MID	Site	123.48	<0.0001	AIG > PED > ORD	285.01	<0.0001	AIG > PED > ORD
	Time	0.006	0.94		192.76	<0.0001	
	Site* Time	5.48	0.008		33.83	<0.0001	
$\delta^{18}O$	Site	169.9	<0.0001	AIG > ORD = PED	499.34	<0.0001	AIG > ORD = PED
	Time	1.1	0.3		1.27	0.26	
	Site* Time	2.2	0.12		7.24	0.0008	
iWUE	Site	104.4	<0.0001	PED = AIG > ORD	419.96	<0.0001	PED > AIG > ORD
	Time	10.4	0.002		643.9	<0.0001	
	Site* Time	1.13	0.33		84.89	<0.0001	

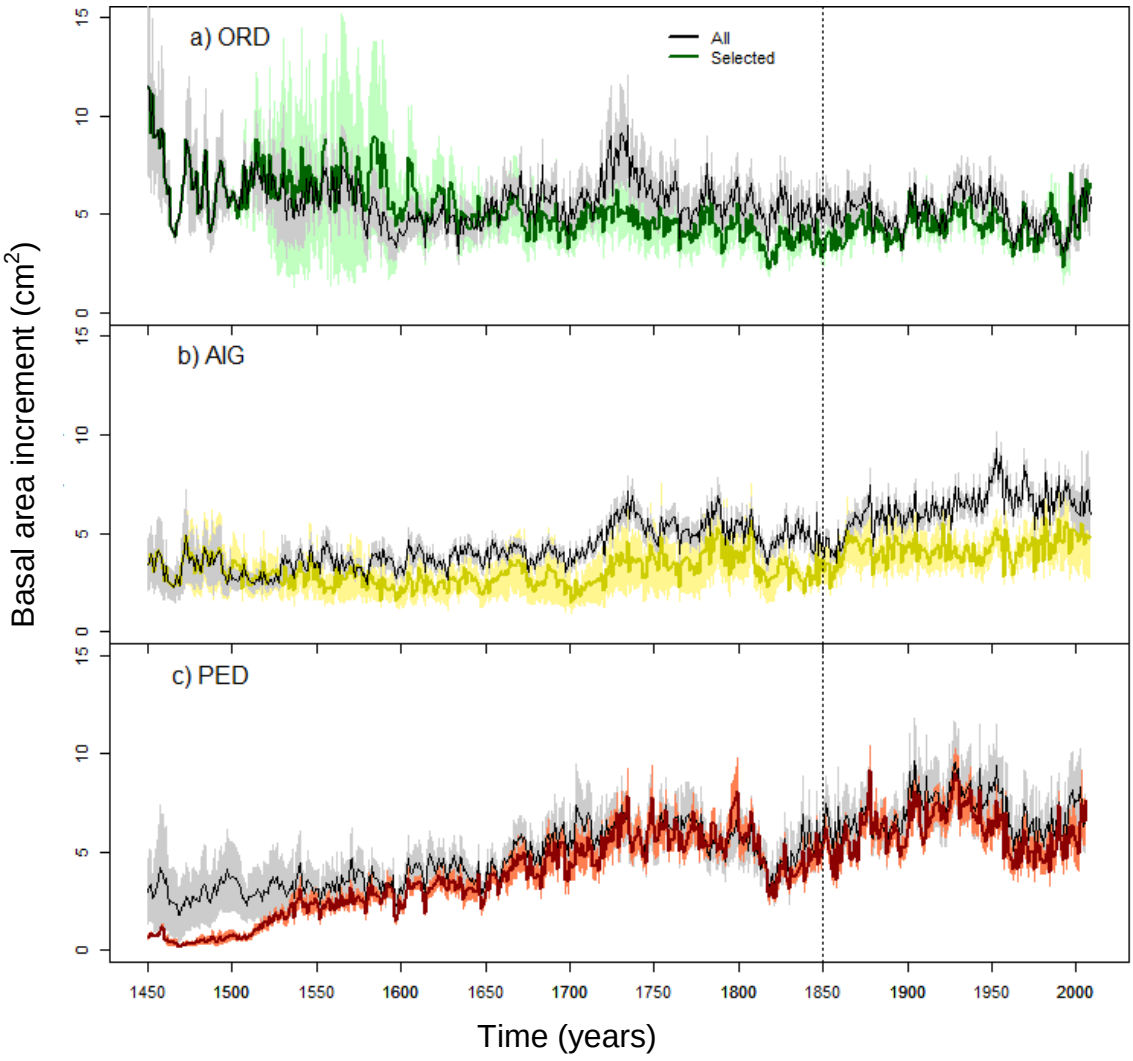

Figure 2. Mean annual basal area increment for the period 1450-2008 of the selected old Mountain pine trees (colored lines) and mean of all individuals older than 400 years at each site (black lines) for the three study sites (a) ORD, b) AIG and c) PED). Colored and gray areas are the SEs of the mean of selected and all trees, respectively. The dotted vertical line indicates the beginning of the industrial period (1850-2008).

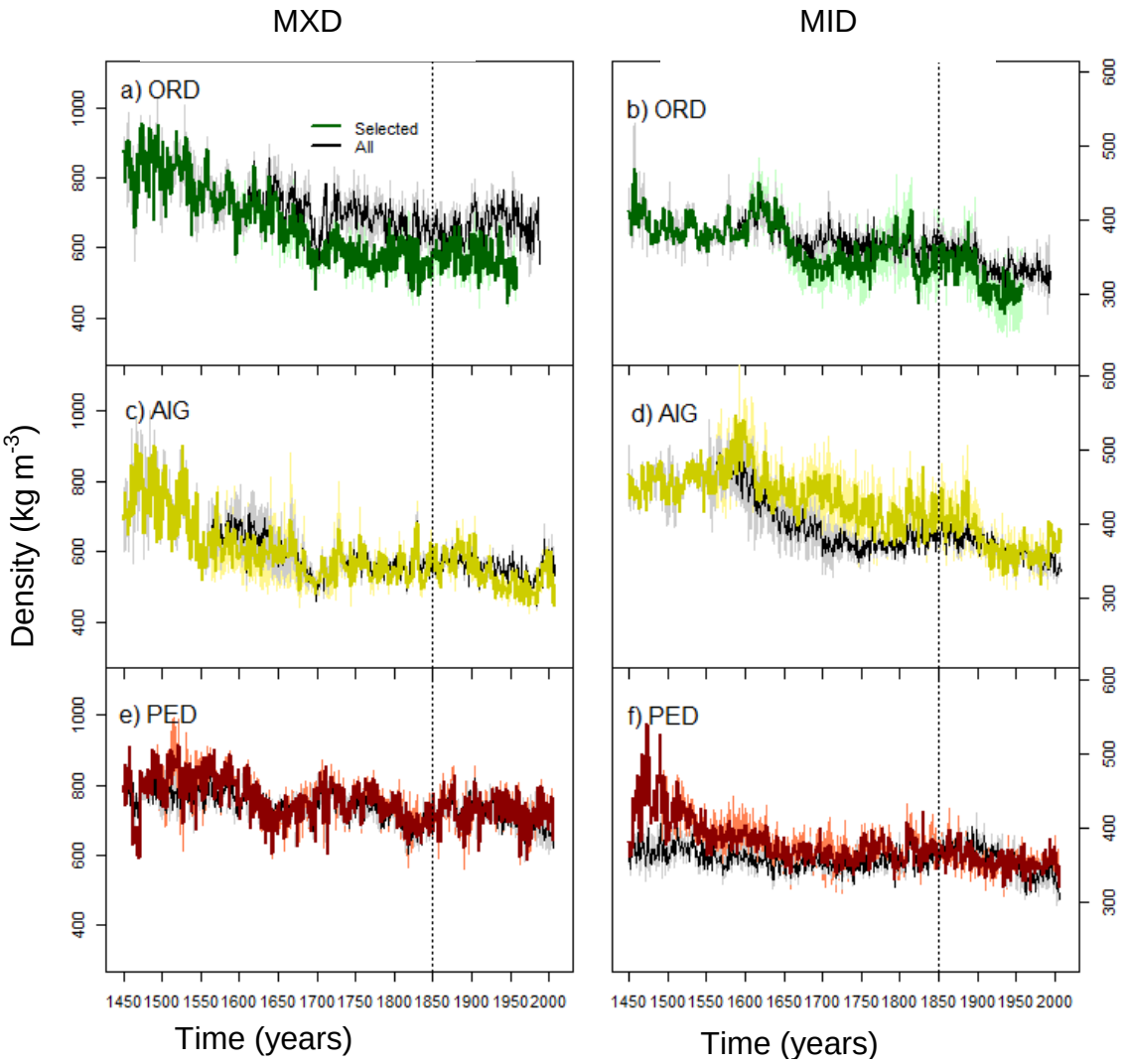

Figure 3. Mean annual maximum (MXD, a, c, e) and minimum (MID, b, d, f) wood density values for the 1450-2008 period considering the selected Mountain pine old trees (represented with colored lines) in relation with all measured individuals (black lines) at each of the three study sites: ORD (a, b), AIG (c, d) and PED (e, f). Colored and gray areas are the SEs of the mean of selected and all trees, respectively. The dotted vertical lines indicate the beginning of the industrial period (1850-2008).

3.2. Oxygen isotope composition and intrinsic water use efficiency

Stable $\delta^{18}O$ trends were found at all sites since 1700 till 1850 (Table 2), and different trends in the industrial period were found over time due to $\delta^{18}O$ increases at PED observed since the 1960s (Table 3, Fig. 4a). Interestingly, $\delta^{18}O$ showed positive correlations with spring and,

386 specially, summer temperatures only at PED (Fig. S2d in Supporting Information), and also
387 negative correlations with precipitation during the same seasons, indicating that increased $\delta^{18}O$
388 was related to warmer and drier conditions during the growing season only at the driest site.

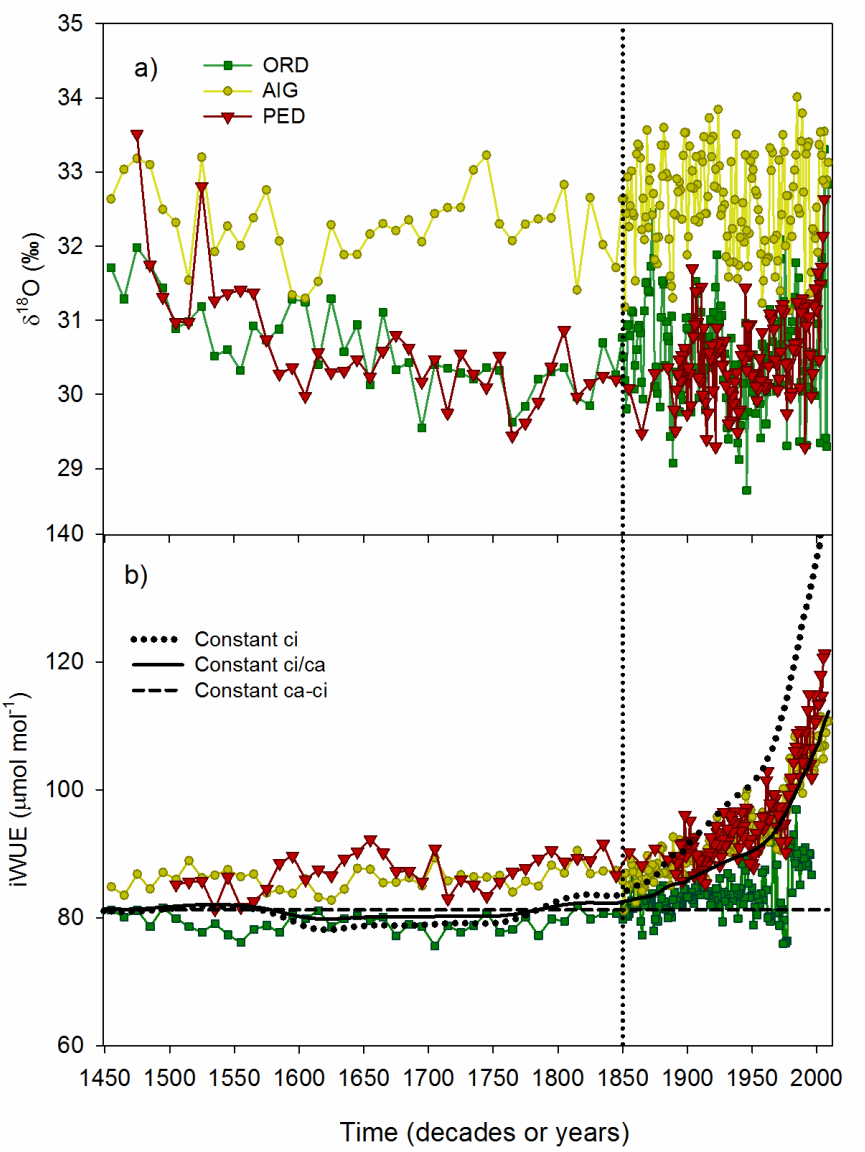

389

390 **Figure 4.** Long-term changes of oxygen isotope ratios (a, $\delta^{18}O$) and intrinsic water use efficiency
391 (b, iWUE) for the 1450-2008 period considering old Mountain pine trees from ORD, AIG and
392 PED study sites. Decadal means are provided for the 1450-1849 period (1450-1889 for PED) and
393 annual values are shown for the industrial period (1850-2008; 1890-2006 for PED). In panel b)
394 the three simulated scenarios according to the different theoretical regulation of plant gas
395 exchange that can occur at increasing atmospheric CO_2 concentrations (c_a) are shown: a constant
396 intercellular CO_2 mole fraction (c_i), a constant c_i/c_a and a constant c_a-c_i. These theoretical

scenarios were compared with iWUE values taken from tree ring $\delta^{13}C$ in trees of the three study sites (ORD, AIG and PED). The dotted vertical line indicates the beginning of the industrial period (1850-2008).

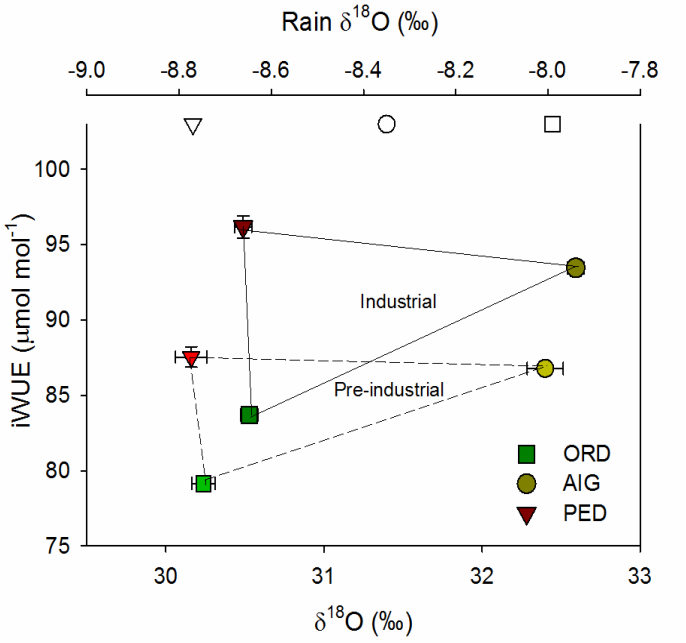

Figure 5. Relationship between oxygen isotope ratios ($\delta^{18}O$) and intrinsic water use efficiency (iWUE) among sites for the two different periods: pre-industrial (1700-1849, dashed line, lighter colors) and industrial period (1850-2008, continuous lines, darker colors). The three sites within each period are connected and the significant differences among variables are provided in Table 3 (pre-industrial vs. industrial periods) and in Table 2 (site differences). Rain $\delta^{18}O$ for each site (see also Table 1) is represented in the x-axis on top by different symbols representing each site (square, ORD; circle, AIG and triangle, PED).

iWUE slightly increased during the pre-industrial period (Table 2), but such increases were more pronounced in the industrial period, especially at AIG and PED (Fig. 4b). Overall, changes in iWUE were consistent with a constant c_i/c_a scenario (AIG: RMSPD at constant c_i = 14.22; constant c_i/c_a = 2.97, constant c_a-c_i =10.02; PED: RMSPD at constant c_i = 13.63; constant c_i/c_a = 3.49, constant c_a-c_i = 12.85), with the exception of ORD, which behaved closer to a constant c_a-c_i scenario (RMSPD at constant c_i = 39.23; constant c_i/c_a = 28.47, constant c_a-c_i = 21.06). At the latter site, however, an increasing trend in iWUE emerged from 1980 onwards (Fig. 4b).

Table 3. Mean and standard error (SE) of the study variables for trees at ORD, AIG and PED sites before and after the industrialization: pre-industrial (1700-1849, decadal values) and industrial (1850-2008, annual values) periods. Positive and negative trends at $P < 0.05$ are indicated by (+) and (-), respectively and non-significant trends by (ns). The last two columns show *t*-test resulting from the comparison between the industrial and pre-industrial periods, with positive *t* values indicating higher values for the industrial than for the pre-industrial period, and negative *t* values indicating lower values for the industrial than for the pre-industrial period.

		Pre-industrial period (1700-1849)			Industrial period (1850-2008)				
Site		Mean	SE	Trend	Mean	SE	Trend	*t* test	*P* value
ORD	BAI	4.29	0.15	-	4.43	0.07	+	0.8	0.43
	MXD	575.05	5.84	-	552.44	5.2	-	-2.89	0.006
	MID	349.17	3.84	ns	305.42	2.88	-	-9.11	<0.0001
	$\delta^{18}O$	30.20	0.07	ns	30.56	0.06	ns	3.89	0.0004
	iWUE	79.18	0.43	+	83.69	0.29	+	8.83	<0.0001
AIG	BAI	3.32	0.17	ns	4.21	0.05	+	5.13	<0.0001
	MXD	554.47	3.94	ns	537.59	4.06	-	-3.08	0.003
	MID	415.28	3.77	-	377.11	2.07	-	-8.27	<0.0001
	$\delta^{18}O$	32.38	0.12	ns	32.59	0.05	ns	1.64	0.12
	iWUE	86.95	0.42	ns	93.42	0.55	+	9.48	<0.0001
PED	BAI	5.27	0.21	ns	6.18	0.1	ns	3.81	0.0009
	MXD	740.32	9.75	-	723.19	3.95	ns	-1.62	0.12
	MID	365.8	2.28	ns	351.7	1.2	-	-5.48	<0.0001
	$\delta^{18}O$	30.16	0.09	ns	30.49	0.05	+	2.93	0.007
	iWUE	87.54	0.67	ns	96.19	0.74	+	8.61	<0.0001

Variables' abbreviations are: basal area increment (BAI, $cm^2\ yr^{-1}$); maximum wood density (MXD, $Kg\ m^3$); minimum wood density (MID, $Kg\ m^3$); oxygen composition ($\delta^{18}O$, ‰) and intrinsic water use efficiency (iWUE, $\mu mol\ mol^{-1}$).

427 *3.3. Differences among sites*

428 Highly positive correlations among old trees were found at the site level for BAI (r = 0.62 –
429 0.96) and wood density (MXD and MID, r = 0.58 – 0.94) (see Table S2 in Supporting
430 Information). Therefore, we assumed that the selected aged trees adequately represent the study
431 populations in these old forests (Figs. 2, 3). For the whole study period the highest BAI and
432 MXD values were observed at PED and the lowest values at AIG (Table 2, Figs. 2, 3). Old trees
433 at ORD exhibited similar BAI to those from AIG in the industrial period (i.e. 1850-2008). The
434 highest MID was found at AIG, followed by PED and ORD (Table 2, Fig. 3). The wood $\delta^{18}O$
435 was higher at AIG than at PED and ORD, which showed similar values (Table 2, Figs. 4a, 5).
436 During the pre-industrial period (1700-1849) PED and AIG trees showed similar iWUE, being
437 higher than ORD trees. During the industrial period PED trees showed the highest iWUE (96.19
438 ± 0.74 µmol mol^{-1}), followed by AIG (93.42 ± 0.55 µmol mol^{-1}) and ORD trees (83.69 ± 0.29
439 µmol mol^{-1}), which also displayed the lowest iWUE during the whole study period (Tables 2, 3;
440 Figs. 4b, 5).

441

442 *3.4. Relationships between variables*

443 During the pre-industrial period the study variables were almost always uncorrelated (Table 4).
444 Two exceptions were found: a negative correlation between BAI and iWUE at ORD, which is
445 overall the result of a slight increase in iWUE coupled with decreased BAI; and a negative
446 correlation between BAI and MID at AIG, which was also significant during the industrial
447 period (Table 4). In this period (1850-2008) we found that BAI and MID were positively
448 correlated with MXD at all sites (Table 4). MXD and $\delta^{18}O$ were also positively correlated, being
449 this relationship stronger at PED. Instead, BAI and iWUE were not positively related, contrary to

expectations (Fig. 1). Interestingly, a positive correlation between $\delta^{18}O$ and iWUE was found only at PED. Through moving correlation analysis (Fig. 6) we found that this positive relationship emerged at this warmest and driest site in the 1960s, thus pointing to stomatal closure driving the observed changes in iWUE.

Table 4. Pearson correlation coefficients among the mean study variables from selected trees at the study sites (ORD, AIG and PED) for two periods: pre-industrial (1700-1849, decadal values) and industrial (1850-2008, annual values) periods. In bold are the significant correlations at the 95% level and grey filling represents significant correlations at 99%.

		Pre-industrial period (1700-1849)				Industrial period (1850-2008)			
Site	Variable	BAI	MID	MXD	$\delta^{18}O$	BAI	MID	MXD	$\delta^{18}O$
ORD	MID	-0.39				**-0.17**			
	MXD	0.57	0.17			**0.41**	**0.16**		
	$\delta^{18}O$	0.12	-0.04	0.02		0.10	-0.04	**0.19**	
	iWUE	**-0.76**	0.32	-0.13	-0.08	**-0.17**	0.04	-0.04	0.02
AIG	MID	**-0.81**				**-0.25**			
	MXD	0.28	-0.06			**0.19**	**0.58**		
	$\delta^{18}O$	0.33	-0.08	0.14		0.03	-0.01	**0.16**	
	iWUE	-0.46	0.43	-0.32	-0.35	0.10	-0.06	-0.03	0.03
PED	MID	0.06				-0.13			
	MXD	0.40	-0.24			**0.43**	**0.33**		
	$\delta^{18}O$	0.20	-0.39	-0.11		0.15	0.03	**0.31**	
	iWUE	0.08	0.33	-0.37	0.20	-0.02	0.13	**0.17**	**0.28**

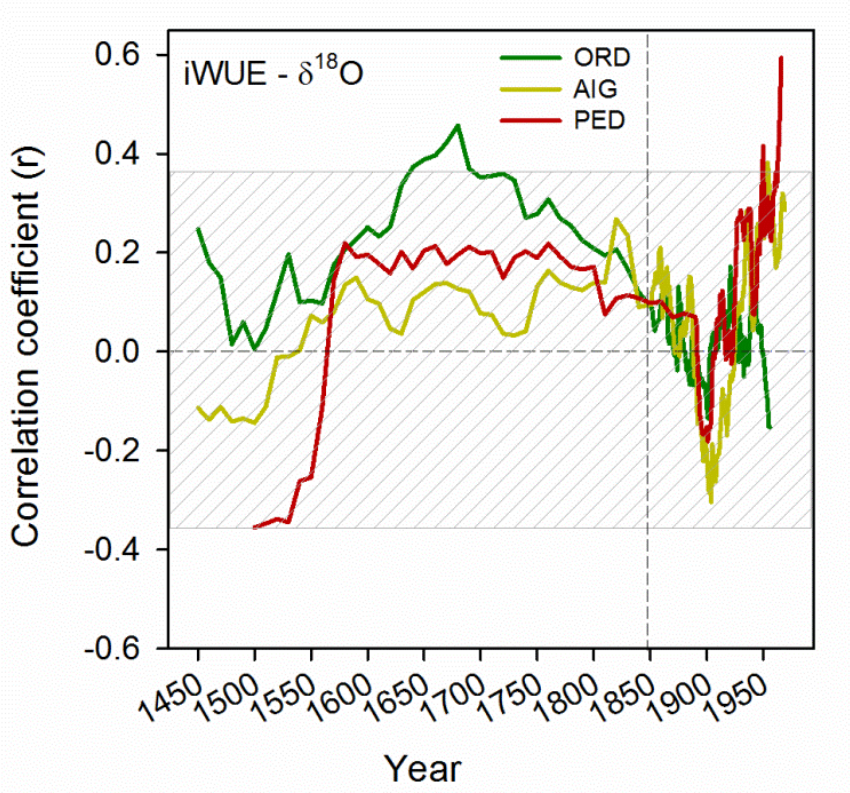

Figure 6. Moving correlation coefficients calculated among intrinsic water-use efficiency (iWUE) and oxygen isotope composition ($\delta^{18}O$) during the study period (we used 40- year moving windows lagged by one year) for ORD, AIG and PED sites. The year in x-axis corresponds to the first year of the 40-year long windows. The horizontal dashed-gray lines represent the 99% confidence intervals. The dashed vertical line indicates the beginning of the industrial period (1850-2008).

4. Discussion

This study assessed long-term productivity and physiological performance of old Mountain pines inhabiting high-elevation forests subjected to cold temperatures. Such assesment was carried out over five centuries through the combined analyses of oxygen isotope ratios ($\delta^{18}O$) and $\Delta^{13}C$-based intrinsic water use efficiency (iWUE), together with growth and wood density as productivity indicators. Overall, our results show that old trees continued to accumulate carbon as wood during the industrial period in spite of being older than 400 years, although probably at

476 lower rates given the slight decreases in wood density observed over this period. Even if some
477 periods exhibited declining growth, the overall positive BAI trends from 1850 to 2008 do not
478 support those studies considering old forests as carbon neutral (Yoder et al. 1994); rather the
479 opposite, we conclude that old trees remain active carbon sinks (Carey et al. 2001; Luyssaert et
480 al. 2008; Stephenson et al. 2014). Increased growth of high-elevation conifer forests has been
481 observed also in other mountain ranges and atributted to increased temperatures and an extended
482 growing season enhancing net photosynthesis in these cold-limited ecosystems (Rolland et al.
483 1998; Salzer et al. 2009; Corona et al. 2015).

484 Despite the outlined long-term growth increase some exceptions were found, most of
485 them punctual decreases coinciding with cold periods. Growth reductions may be determined by
486 changes in air temperatures directly driving tissue formation (e.g. cell division and expansion),
487 processes that have been shown to be more sensitive to low temperatures than photosynthesis
488 (Körner 2003; Rossi et al. 2008; Körner 2012). In agreement, during the same cold periods (e.g,
489 1810s-1830s and 1970s) wood density also dropped. Reductions in MXD, whose variability is
490 related to processes involved in biomass acumulation during the late growing season such as
491 cell-wall thickening and lignification, could also be due to declines in carbon supply and
492 partitioning (Thomas et al. 2007) if low temperatures result in photoinhibition (Adams III et al.
493 1994; Murata et al. 2007).

494 Xylem anatomical traits, and thus wood density, are related to carbon fixation but also to
495 water exchange (Hacke et al. 2001). Specifically, while MXD provides more information about
496 the carbon allocation to tracheid cell walls during the late growing season, the minimum wood
497 density (MID) is more informative of the hydraulic conditions during the early growing season
498 when radial-growth rates peak (Camarero et al. 2014). Our results point to a generalized

499 declining trend in wood density, at least from 1450 to 1700, which could reflect ontogenetic
500 effects related e.g. to the transition from more dense heartwood to less dense sapwood (Chave et
501 al. 2009) and the formation of younger tracheids with wider lumen areas from the pith towards
502 the bark (Anfodillo et al. 2013; Carrer et al. 2015). Positive correlations between growth and
503 MXD and between MXD and MID were mainly found after 1850. This suggests a consistent
504 effect of temperature, as shown by positive correlations with these wood traits (Fig. S2). MXD in
505 high-elevation conifer forests and in other cold habitats (e.g. boreal forests) has been shown to be
506 highly sensitive to temperatures during the late growing season (e.g, Büntgen et al. 2008),
507 integrating influences from meteorological conditions over much of the growing season by
508 assimilates deposition in cell walls. The positive relationships between MXD and $\delta^{18}O$ could
509 also reflect a common controling factor such as temperature rather than a causal relationship.
510 Interestingly, higher growth coupled with lower MID was especially found in AIG, the site with
511 the highest MID values. We hypothesize that the AIG old trees bearing the lowest conduit area
512 are the most potentially benefitted by climate warming through growth enhancement, the
513 production of wider tracheid lumens and an improved hydraulic conductivity (Hacke et al. 2001;
514 Ziaco et al. 2014). Non-significant correlations were found between iWUE and density traits,
515 which points to a general independence of tracheid lumen area and carbon allocation to cell walls
516 from iWUE, except at PED. Olano et al. (2014) also found a lack of correlation between
517 conductive traits and iWUE in *Juniperus thurifera* but they reported negative relationships
518 between iWUE and cell-wall thickness. Instead, our results point to higher wall thickness with
519 greater iWUE at PED, likely due to higher C allocation to cell walls (Babst et al. 2014b).

520 A lack of significant positive relationships between radial growth and iWUE was found
521 during the industrial period. As a consequence, the substantial enhancement in iWUE since 1850

caused by c_a increase is unlikely responsible for the generalized growth enhancement (Andreu-Hayles et al. 2011). Non-significant or negative relationships between iWUE and growth are commonly explained as a predominant influence of stressors (e.g. increasing drought stress leading to stomatal closure) whose effects override any potential c_a fertilization on tree growth (Peñuelas et al. 2011; Silva et al. 2013; Levesque et al. 2014; Liu et al. 2014; Camarero et al. 2015c). However, our results derived from $\delta^{18}O$ records did not report general reductions in g_s, which will be the primary response to drought, likely due to the wet and cold conditions of these high-elevation forests. The exception was found in PED since 1960, when simultaneous increases in $\delta^{18}O$ and iWUE indicate stomatal closure likely due to an emerging climate stress related to increased atmospheric drought (Barbour et al. 2000; Grams et al. 2007). Andreu-Hayles et al. (2011) found similar results and suggested that a decrease of g_s should explain this pattern, now confirmed in the case of PED by the $\delta^{18}O$ trends. Such alteration in the performance of old trees was not observed in the other two sites, which is likely explained by the drier conditions found in PED due to increased temperatures despite the general wet nature of these high-elevation forests. In fact, the decreased g_s related to higher temperatures and lower precipitation during the growing season was only found in the PED forest (Fig. S2) supporting this climate effect, which is well captured by O and C isotopes (Planells et al. 2005). As a consequence, our results point to an isohydric behaviour (i.e. strict stomatal control to reduce transpiration) under decreasing relative humidity since 1960 and, thus, to stomatal limitation of photosynthesis in old pines from this high-elevation forest (Flexas & Medrano 2002). Importantly, this emerging drought stress has been inferred for other Mountain pine forests based on climate-growth associations, which indicates that climate warming could alter the future growth and functioning of high-elevation cold-limited forests (Galván et al. 2015).

In the case of AIG and ORD sites, the iWUE improvement during the industrial period may be caused by an increase in *A* given that δ^{18}O-derived g_s was maintained rather stable from the 1850s onwards (Scheidegger et al. 2000). Similarly, Fernández-Martínez & Fleck (2016) found increased photosynthetic rates and iWUE for Mountain pine withouth changes in g_s under elevated c_a. Thus, sufficient water availability, higher c_a and warm temperatures may enhance *A* and lead to increased C inputs in these high-elevation forests (Streit et al. 2014). However, the growth- iWUE uncoupling indicates that the photo-assimilates were likely allocated to other aboveground or belowground organs or even stored as non-structural carbohydrates (Palacio et al. 2014). Another possible explanation could be a higher carbon loss resulting from higher respiration rates with increasing temperatures during the industrial period (see also Nock et al. 2010). Thus, the increasing growth during the industrial period would be a consequence of greater meristem activity or an extended wood phenology under warmer temperatures (Körner 2015; Delpierre et al. 2016) rather than the result of enhanced photosynthetic rates.

The differences observed in Mountain pine tree performance among sites highlight that local conditions are relevant to understand the responses of old trees to the changing climate and the rise in c_a. For instance, trees from the warmest and driest site (PED), bearing the highest growth and maximum wood density (MXD) seemed the most stressed during the last decades according to the inferred changes in g_s. Interestingly, although PED and ORD trees had similar wood δ^{18}O values suggesting a comparable g_s, a lower iWUE was found in ORD. Rain δ^{18}O estimated using monthly precipitation and temperature data (Ferrio & Voltas 2005) indicated higher site values in ORD than in PED (Table 1, Fig. 4), which denotes that such similar wood δ^{18}O records observed among study sites were likely the outcome of a higher stomatal control of water losses in PED. Trees from AIG had lower g_s (inferred from higher δ^{18}O despite the

568 intermediate values of rain $\delta^{18}O$) in relation with the other two forests, which could be due to its
569 higher altitude, as shown by Keitel et al. (2006), or related to enhanced humitidy due to its
570 location close to the more humid north-facing French Pyrenees.

571 Lastly, we are aware of possible biases in the interpretation of carbon and oxygen
572 isotopic signatures . For instance, multiple C sources are integrated in tree-ring $\delta^{13}C$, from leaf
573 photoassimilates to stored C pools (Seibt et al. 2008). Furthermore, the use of different source
574 waters along the growing season could be influencing wood $\delta^{18}O$ (Roden & Siegwolf 2012). We
575 further acknowledge that other local factors such as the contrasting nutrient availability in the
576 soil (basic soils in ORD and PED *vs.* acid ones in AIG) could also be responsible for contrasting
577 tree responses at site level given that Mountain pine photosynthesis can be constrained in sites
578 with poor soils and low N concentration (Fernández-Martínez & Fleck 2016). Therefore, growth
579 fertilization could also be expected if N loads increase in the future, albeit current N deposition
580 rates are relatively low in these areas (Badeau et al. 1996; but see Boutin et al. 2015). A higher
581 sample replication and the use of mechanistic approaches based on mutiple isotope
582 measurements in old trees will be further needed to test our findings and to evaluate the
583 applicability of our interpretations.

584 To conclude, we have shown that old Mountain pine trees continue accumulating carbon
585 as woody biomass. Warmer temperatures in these cold-limited ecosystems are enhancing or
586 sustaining growth of aged trees in the study high-elevation old forests. It is plausible that climate
587 warming in these cold environments is enhancing growth thanks to a greater meristem activity
588 during a longer growing season. Positive correlations between growth and maximum wood
589 density suggest a consistent effect of temperature on both traits. During the industrial period the
590 uncoupling between growth and rising iWUE was not due to a reduced stomatal conductance,

591 and it could be explained because increased photosynthetic rates did not translate into greater
592 growth but into carbon allocation to other organs. In the driest site instead, a strong stomatal
593 control to reduce transpiration under decreasing relative humidity was found in recent decades,
594 which suggests that drought stress could be emerging in some of these high-elevation forests if
595 they are subjected to progressively warm and dry conditions.
596

597 ## *5. Acknowledgements*

598 We are very grateful to several projects financed by "Organismo Autónomo de Parques
599 Nacionales" (projects 12/2008 387/2011). E.G. was funded by a Juan de la Cierva post-doctoral
600 research contract (FJCI-2014-19615, MEC, Spain). Spanish (AMB95-0160, CGL2011-26654)
601 and EU projects ISONET (contract EV K2-2001-00237) and MILLENNIUM (017008–2) also
602 supported this study by contributing additional datasets.
603
604
605

606 *6. References*
607

608 Adams III, W.W., Demmig-Adams, B., Verhoeven, A.S. & Barker, D.H. (1994) 'Photoinhibition'
609 during winter stress: involvement of sustained xanthophyll cycle-dependent energy
610 dissipation. *Australian Journal of Plant Physiology,* **22,** 261-276.
611 Agustí-Panareda, A., Thompson, R. & Livingstone, D.M. (2000) Reconstructing temperature
612 variations at high elevation lake sites in Europe during the instrumental period. *Verh. Int.*
613 *Ver. Limn,* **27,** 479–483.
614 Andreu-Hayles, L., Planells, O., Gutiérrez, E., Muntan, E., Helle, G., Anchukaitis, K.J. &
615 Schleser, G.H. (2011) Long tree-ring chronologies reveal 20th century increases in water-
616 use efficiency but no enhancement of tree growth at five Iberian pine forests. *Global*
617 *Change Biology,* **17,** 2095-2112.
618 Anfodillo, T., Petit, G. & Crivellaro, A. (2013) Axial conduit widening in woody species: a still
619 neglected anatomical pattern. *Iawa Journal,* **34,** 352-364.
620 Babst, F., Alexander, M.R., Szejner, P., Bouriaud, O., Klesse, S., Roden, J., Ciais, P., Poulter, B.,
621 Frank, D., Moore, D.J. & Trouet, V. (2014a) A tree-ring perspective on the terrestrial
622 carbon cycle. *Oecologia,* **176,** 307-322.
623 Babst, F., Bouriaud, O., Papale, D., Gielen, B., Janssens, I.A., Nikinmaa, E., Ibrom, A., Wu, J.,
624 Bernhofer, C., Kostner, B., Grunwald, T., Seufert, G., Ciais, P. & Frank, D. (2014b)
625 Above-ground woody carbon sequestration measured from tree rings is coherent with net
626 ecosystem productivity at five eddy-covariance sites. *New Phytologist,* **201,** 1289-1303.
627 Badeau, V., Becker, M., Bert, D., Dupouey, J.-L., Lebourgeois, F. & Picard, J.-F. (1996) Long-
628 term growth trends of trees: ten years of dendrochronological studies in France. *Growth*
629 *trends in European forests* (eds H. Spiecker, K. Mielikäinen, M. Köhl & J.P.
630 Skovsgaard), pp. 167–181. Springer, Berlin.
631 Barbour, M.M., Fischer, R.A., Sayre, K.D. & Farquhar, G.D. (2000) Oxygen isotope ratio of leaf
632 and grain material correlates with stomatal conductance and grain yield in irrigated
633 wheat. *Australian Journal of Plant Physiology,* **27,** 625-637.
634 Barbour, M.M., Walcroft, A.S. & Farquhar, G.D. (2002) Seasonal variation in d13C and d18O of
635 cellulose from growth rings of *Pinus radiate. Plant, Cell and Environment,* **25,** 1483-
636 1499.
637 Biondi, F. & Qeadan, F. (2008) A theory-driven approach to tree-ring standarization: defining
638 the biological trend from expected basal area increment. *Tree-Ring Research,* **64,** 81-96.
639 Bouriaud, O., Teodosiu, M., Kirdyanov, A.V. & Wirth, C. (2015) Influence of wood density in
640 tree-ring based annual productivity assessments and its errors in Norway spruce.
641 *Biogeosciences Discussions,* **12,** 5871-5905.
642 Boutin, M., Lamaze, T., Couvidat, F. & Pornon, A. (2015) Subalpine Pyrenees received higher
643 nitrogen deposition than predicted by EMEP and CHIMERE chemistry-transport models.
644 *Scientific Reports,* **5,** 12942.
645 Büntgen, U., Frank, D., Grudd, H. & Esper, J. (2008) Long-term summer temperature variations
646 in the Pyrenees. *Climate Dynamics,* **31,** 615-631.
647 Camarero, J.J., Gazol, A., Galvan, J.D., Sanguesa-Barreda, G. & Gutiérrez, E. (2015a) Disparate
648 effects of global-change drivers on mountain conifer forests: warming-induced growth
649 enhancement in young trees vs. CO_2 fertilization in old trees from wet sites. *Global*
650 *Change Biology,* **21,** 738-749.

Camarero, J.J., Gazol, A., Sangüesa-Barreda, G., Oliva, J., Vicente-Serrano, S.M. & Gibson, D. (2015b) To die or not to die: early warnings of tree dieback in response to a severe drought. *Journal of Ecology,* **103,** 44-57.

Camarero, J.J., Gazol, A., Tardif, J.C. & Conciatori, F. (2015c) Attributing forest responses to global-change drivers: limited evidence of a CO_2-fertilization effect in Iberian pine growth. *Journal of Biogeography,* **42,** 2220-2233.

Camarero, J.J., Guerrero-Campo, J. & Gutierrez, E. (1998) Tree-ring growth and structure of *Pinus uncinata* and *Pinus sylvestris* in the Central Spanish Pyrenees. *Arctic and Alpine Research,* **30,** 1-10.

Camarero, J.J. & Gutiérrez, E. (1999) Structure and recent recruitment at alpine forest-pasture ecotones in the Spanish central Pyrenees. *Ecoscience,* **6,** 451-464.

Camarero, J.J., Rozas, V., Olano, J.M. & Fernández-Palacios, J.M. (2014) Minimum wood density of *Juniperus thurifera* is a robust proxy of spring water availability in a continental Mediterranean climate. *Journal of Biogeography,* **41,** 1105-1114.

Carey, E.V., Sala, A., Keane, R. & Callaway, R.M. (2001) Are old forests underestimated as global carbon sinks? *Global Change Biology,* **7,** 339-344.

Carrer, M., von Arx, G., Castagneri, D. & Petit, G. (2015) Distilling allometric and environmental information from time series of conduit size: the standardization issue and its relationship to tree hydraulic architecture. *Tree Physiology,* **35,** 27-33.

Chave, J., Coomes, D., Jansen, S., Lewis, S.L., Swenson, N.G. & Zanne, A.E. (2009) Towards a worldwide wood economics spectrum. *Ecology Letters,* **12,** 351-366.

Choury, Z., Shestakova, T., Himrane, H., Touchan, R., Kherchouche, D., Camarero, J.J. & Voltas, J. (2017) Quarantining the Sahara desert: growth and water-use efficiency of Aleppo pine in the Algerian Green Barrier. *European Journal of Forest Research*. doi: 10.1007/s10342-016-1014-3

Churakova Sidorova, O.V., Saurer, M., Bryukhanova, M.V., Siegwolf, R.T. & Bigler, C. (2016) Site-specific water-use strategies of mountain pine and larch to cope with recent climate change. *Tree Physiology,* **36,** 942-953.

Corona, C., López-Sáez, J., Stoffel, M., Rovréra, G., Edouard, J.-L. & Guibal, F. (2015) Impacts of more frequent droughts on a relict low-altitude *Pinus uncinata* stand in the French Alps. *Frontiers in Ecology and Evolution,* **2**. doi: 10.3389 /fevo.2014.00082.

Delpierre, N., Berveiller, D., Granda, E. & Dufrene, E. (2016) Wood phenology, not carbon input, controls the interannual variability of wood growth in a temperate oak forest. *New Phytologist,* **210,** 459-470.

Dorado Liñán, I., Büntgen, U., González-Rouco, F., Zorita, E., Montávez, J.P., Gómez-Navarro, J.J., Brunet, M., Heinrich, I., Helle, G. & Gutiérrez, E. (2012) Estimating 750 years of temperature variations and uncertainties in the Pyrenees by tree-ring reconstructions and climate simulations. *Climate of the Past,* **8,** 919-933.

Duncan, R.P. (1989) An evaluation of errors in tree age estimates based on increment cores in Kahikatea (*Dacrycarpus dacrydioides*) *New Zeland Natural Sciences,* **16,** 31-37.

Fardusi, M.J., Ferrio, J.P., Comas, C., Voltas, J., Resco de Dios, V. & Serrano, L. (2016) Intra-specific association between carbon isotope composition and productivity in woody plants: A meta-analysis. *Plant Science,* **251,** 110-118.

Farquhar, G.D., Oleary, M.H. & Berry, J.A. (1982) On the relationship between carbon isotope discrimination and the inter-cellular crabon-dioxide concentration in leaves. *Australian Journal of Plant Physiology,* **9,** 121-137.

Farquhar, G.D. & Richards, R. (1984) Isotopic composition of plant carbon correlates with water-use efficiency of wheat genotypes. *Australian Journal of Plant Physiology,* **11,** 539-552.

Fernández-Martínez, J. & Fleck, I. (2016) Photosynthetic limitations of several representative sub-alpine species in the Catalan Pyrenees during the summer. *Plant Biology*. doi: 10.1111/plb.12439

Ferrio, J.P. & Voltas, J. (2005) Carbon and oxygen isotope ratios in wood constituents of *Pinus halepensis* as indicators of precipitation, temperature and vapour pressure deficit. *Tellus Series B-Chemical and Physical Meteorology,* **57,** 164-173.

Flexas, J. & Medrano, H. (2002) Drought-inhibition of photosynthesis in C3 plants: stomatal and non-stomatal limitations revisited. *Annals of Botany,* **89,** 183-189.

Galván, J.D., Büntgen, U., Ginzler, C., Grudd, H., Gutiérrez, E., Labuhn, I. & Camarero, J.J. (2015) Drought-induced weakening of growth–temperature associations in high-elevation Iberian pines. *Global and Planetary Change,* **124,** 95-106.

Galván, J.D., Camarero, J.J., Gutiérrez, E. & Zuidema, P. (2014) Seeing the trees for the forest: drivers of individual growth responses to climate in *Pinus uncinata* mountain forests. *Journal of Ecology,* **102,** 1244-1257.

Grams, T.E., Kozovits, A.R., Haberle, K.H., Matyssek, R. & Dawson, T.E. (2007) Combining delta ^{13} C and delta ^{18} O analyses to unravel competition, CO_2 and O_3 effects on the physiological performance of different-aged trees. *Plant Cell and Environment,* **30,** 1023-1034.

Grudd, H. (2008) Torneträsk tree-ring width and density ad 500–2004: a test of climatic sensitivity and a new 1500-year reconstruction of north Fennoscandian summers. *Climate Dynamics,* **31,** 843-857.

Gunderson, C.A., O'Hara, K.H., Campion, C.M., Walker, A.V. & Edwards, N.T. (2010) Thermal plasticity of photosynthesis: the role of acclimation in forest responses to a warming climate. *Global Change Biology,* **16**, 2272-2286.

Hacke, U.G., Sperry, J.S., Pockman, W.T., Davis, S.D. & McCulloh, K.A. (2001) Trends in wood density and structure are linked to prevention of xylem implosion by negative pressure. *Oecologia,* **126,** 457-461.

Harris, I., Jones, P.D., Osborn, T.J. & Lister, D.H. (2014) Updated high-resolution grids of monthly climatic observations - the CRU TS3.10 Dataset. *International Journal of Climatology,* **34,** 623-642.

Holmes, R.L. (1983) Computer-assisted quality control in tree-ring dating and measurement. *Tree-Ring Bulletin,* **43,** 69-78.

Huang, J.G., Bergeron, Y., Denneler, B., Berninger, F. & Tardif, J. (2007) Response of forest trees to increased atmospheric CO_2. *Critical Reviews in Plant Sciences,* **26,** 265-283.

IPCC (2014) *Climate change 2014: Mitigation of climate change. Contribution of Working Group III to the fifth assessment report of the Intergovernmental Panel on Climate Change*. Cambridge University Press, Cambridge, UK & New York, NY, USA.

Keitel, C., Matzarakis, A., Rennenberg, H. & Gessler, A. (2006) Carbon isotopic composition and oxygen isotopic enrichment in phloem and total leaf organic matter of European beech (*Fagus sylvatica* L.) along a climate gradient. *Plant, Cell and Environment,* **29,** 1492-1507.

Körner, C. (2003) Carbon limitation in trees. *Journal of Ecology,* **91,** 4-17.

Körner, C. (2012) *Alpine treelines*. Springer, Basel.

Körner, C. (2015) Paradigm shift in plant growth control. *Current Opinion in Plant Biology*, **25,** 107-114.
Körner, C. (2017) A matter of tree longevity. *Science*, **355**, 130-131.
Leavitt, S.W. & Danzer, S.R. (1993) Method for batch processing small wood samples to holocellulose for stable-carbon isotipe analysis. *Analytical Chemistry*, **65,** 87-89.
Levesque, M., Siegwolf, R., Saurer, M., Eilmann, B. & Rigling, A. (2014) Increased water-use efficiency does not lead to enhanced tree growth under xeric and mesic conditions. *New Phytologist*, **203,** 94-109.
Liu, X., Wang, W., Xu, G., Zeng, X., Wu, G., Zhang, X. & Qin, D. (2014) Tree growth and intrinsic water-use efficiency of inland riparian forests in northwestern China: evaluation via delta^{13}C and delta^{18}O analysis of tree rings. *Tree Physiology*, **34,** 966-980.
López-Moreno, J.I., Goyette, S. & Beniston, M. (2008) Climate change prediction over complex areas: spatial variability of uncertainties and predictions over the Pyrenees from a set of regional climate models. *International Journal of Climatology*, **28,** 1535-1550.
Luyssaert, S., Schulze, E.D., Borner, A., Knohl, A., Hessenmoller, D., Law, B.E., Ciais, P. & Grace, J. (2008) Old-growth forests as global carbon sinks. *Nature*, **455,** 213-215.
McCarroll, D. & Loader, N.J. (2004) Stable isotopes in tree rings. *Quaternary Science Reviews*, **23,** 771-801.
Mencuccini, M. (2002) Hydraulic constraints in the functional scaling of trees. *Tree Physiology*, **22,** 553-565.
Mencuccini, M., Martinez-Vilalta, J., Vanderklein, D., Hamid, H.A., Korakaki, E., Lee, S. & Michiels, B. (2005) Size-mediated ageing reduces vigour in trees. *Ecology Letters*, **8,** 1183-1190.
Murata, N., Takahashi, S., Nishiyama, Y. & Allakhverdiev, S.I. (2007) Photoinhibition of photosystem II under environmental stress. *Biochimica et Biophysica Acta*, **1767,** 414-421.
Nock, C.A., Baker, P.J., Wanek, W., Leis, A., Grabner, M., Bunyavejchewin, S. & Hietz, P. (2010) Long-term increases in intrinsic water-use efficiency do not lead to increased stem growth in a tropical monsoon forest in western Thailand. *Global Change Biology*, **17,** 1049-1063.
Olano, J.M., Linares, J.C., Garcia-Cervigon, A.I., Arzac, A., Delgado, A. & Rozas, V. (2014) Drought-induced increase in water-use efficiency reduces secondary tree growth and tracheid wall thickness in a Mediterranean conifer. *Oecologia*, **176,** 273-283.
Palacio, S., Hoch, G., Sala, A., Körner, C. & Millard, P. (2014) Does carbon storage limit tree growth? *New Phytologist*, **201,** 1096–1100.
Pellizzari, E., Camarero, J.J., Gazol, A., Sanguesa-Barreda, G. & Carrer, M. (2016) Wood anatomy and carbon-isotope discrimination support long-term hydraulic deterioration as a major cause of drought-induced dieback. *Global Change Biology*, **22,** 2125-2137.
Peñuelas, J., Canadell, J.G. & Ogaya, R. (2011) Increased water-use efficiency during the 20th century did not translate into enhanced tree growth. *Global Ecology and Biogeography*, **20,** 597-608.
Planells, O., Andreu, L., Bosch, O., Gutiérrez, E., Filot, M., Leuenberger, M., Helle, G. & Schleser, G.H. (2005) The potential of stable isotopes to record aridity conditions in a forest with low-sensitive ring widths from the eastern Pre- Pyrenees. *TRACE-Tree rings in Archaeology, Climatology and Ecology*, **4,** 266-272.

Ponton, S., Dupouey, J.L., Breda, N., Feuillat, F., Bodenes, C. & Dreyer, E. (2001) Carbon isotope discrimination and wood anatomy variations in mixed stands of *Quercus robur* and *Quercus petraea*. *Plant Cell and Environment*, **24**, 861-868.

R Development Core Team (2014) R: A Language and Environment for Statistical Computing. R Foundation for Statistical Computing, Vienna.

Roden, J. & Siegwolf, R. (2012) Is the dual-isotope conceptual model fully operational? *Tree Physiology*, **32,** 1179-1182.

Rolland, C., Petitcolas, V. & Michalet, R. (1998) Changes in radial tree growth for *Picea abies, Larix decidua, Pinus cembra* and *Pinus uncinata* near the alpine timberline since 1750. *Trees-Structure and Function*, **13,** 40-53.

Rossi, S., Deslauriers, A., Anfodillo, T. & Carrer, M. (2008) Age-dependent xylogenesis in timberline conifers. *New Phytologist*, **177,** 199-208.

Ryan, M.G. & Yoder, B.J. (1997) Hydraulic limits to tree height and tree growth. *Bioscience*, **47,** 235-242.

Salzer, M.W., Hughes, M.K., Bunn, A.G. & Kipfmueller, K.F. (2009) Recent unprecedented tree-ring growth in bristlecone pine at the highest elevations and possible causes. *Proceedings of the National Academy of Sciences of the United States of America*, **106,** 20348-20353.

Saurer, M., Borella, S. & Leuenberger, M. (1997) $\delta^{18}O$ of tree rings of beech (*Fagus silvatica*) as a record of d18O of the growing season precipitation. *Tellus B*, **49,** 80-92.

Saurer, M., Siegwolf, R.T.W. & Schweingruber, F.H. (2004) Carbon isotope discrimination indicates improving water-use efficiency of trees in northern Eurasia over the last 100 years. *Global Change Biology*, **10,** 2109-2120.

Saurer, M., Spahni, R., Frank, D.C., Joos, F., Leuenberger, M., Loader, N.J., McCarroll, D., Gagen, M., Poulter, B., Siegwolf, R.T., Andreu-Hayles, L., Boettger, T., Dorado Linan, I., Fairchild, I.J., Friedrich, M., Gutierrez, E., Haupt, M., Hilasvuori, E., Heinrich, I., Helle, G., Grudd, H., Jalkanen, R., Levanic, T., Linderholm, H.W., Robertson, I., Sonninen, E., Treydte, K., Waterhouse, J.S., Woodley, E.J., Wynn, P.M. & Young, G.H. (2014) Spatial variability and temporal trends in water-use efficiency of European forests. *Global Change Biology*, **20,** 3700-3712.

Scheidegger, Y., Saurer, M., Bahn, M. & Siegwolf, R. (2000) Linking stable oxygen and carbon isotopes with stomatal conductance and photosynthetic capacity: a conceptual model. *Oecologia*, **125,** 350-357.

Seibt, U., Rajabi, A., Griffiths, H. & Berry, J.A. (2008) Carbon isotopes and water use efficiency: sense and sensitivity. *Oecologia*, **155,** 441-454.

Silva, L.C. & Horwath, W.R. (2013) Explaining global increases in water use efficiency: why have we overestimated responses to rising atmospheric CO_2 in natural forest ecosystems? *Plos One*, **8,** e53089.

Silva, L.C.R., Anand, M., Oliveira, J.M. & Pillar, V.D. (2009) Past century changes in *Araucaria angustifolia* (Bertol.) Kuntze water use efficiency and growth in forest and grassland ecosystems of southern Brazil: implications for forest expansion. *Global Change Biology*, **15,** 2387-2396.

Silva, L.C.R., Anand, M. & Shipley, B. (2013) Probing for the influence of atmospheric CO_2 and climate change on forest ecosystems across biomes. *Global Ecology and Biogeography*, **22,** 83-92.

Stephenson, N.L., Das, A.J., Condit, R., Russo, S.E., Baker, P.J., Beckman, N.G., Coomes, D.A., Lines, E.R., Morris, W.K., Ruger, N., Alvarez, E., Blundo, C., Bunyavejchewin, S., Chuyong, G., Davies, S.J., Duque, A., Ewango, C.N., Flores, O., Franklin, J.F., Grau, H.R., Hao, Z., Harmon, M.E., Hubbell, S.P., Kenfack, D., Lin, Y., Makana, J.R., Malizia, A., Malizia, L.R., Pabst, R.J., Pongpattananurak, N., Su, S.H., Sun, I.F., Tan, S., Thomas, D., van Mantgem, P.J., Wang, X., Wiser, S.K. & Zavala, M.A. (2014) Rate of tree carbon accumulation increases continuously with tree size. *Nature,* **507,** 90-93.

Stokes, M.A. & Smiley, T.L. (1968) *An Introduction to Tree Ring Dating.* University Chicago Press, Chicago, IL, USA.

Streit, K., Siegwolf, R.T., Hagedorn, F., Schaub, M. & Buchmann, N. (2014) Lack of photosynthetic or stomatal regulation after 9 years of elevated CO_2 and 4 years of soil warming in two conifer species at the alpine treeline. *Plant, Cell and Environment,* **37,** 315-326.

Tardif, J., Camarero, J.J., Ribas, M. & Gutierrez, E. (2003) Spatiotemporal variability in tree growth in the Central Pyrenees: Climatic and site influences. *Ecological Monographs*, **73,** 241-257.

Thomas, D.S., Montagu, K.D. & Conroy, J.P. (2007) Temperature effects on wood anatomy, wood density, photosynthesis and biomass partitioning of *Eucalyptus grandis* seedlings. *Tree Physiology,* **27,** 251-260.

Treydte, K., Boda, S., Graf Pannatier, E., Fonti, P., Frank, D., Ullrich, B., Saurer, M., Siegwolf, R., Battipaglia, G., Werner, W. & Gessler, A. (2014) Seasonal transfer of oxygen isotopes from precipitation and soil to the tree ring: source water versus needle water enrichment. *New Phytologist,* **202,** 772-783.

Voelker, S.L., Muzika, R.M., Guyette, R.P. & Stambaugh, M.C. (2006) Historical CO2 Growth Enhancement Declines with Age in *Quercus* and *Pinus*. *Ecological Monographs,* **76,** 549-564.

Way, D.A. & Oren, R. (2010) Differential responses to changes in growth temperature between trees from different functional groups and biomes: a review and synthesis of data. *Tree Physiology,* **30,** 669-688.

Yoda, K., Shinozaki, K., Ogawa, H., Hozumi, K. & Kira, T. (1965) Estimation of the total amount of respiration in woody organs of trees and forest communities. *Journal of Biology of Osaka City University,* **16,** 15–26.

Yoder, B.J., Ryan, M.G., Waring, R.H., Schoettle, A.W. & Kaufmann, M.R. (1994) Evidence of reduced photosynthetic rates in old trees. *Forest Science,* **40,** 513-527.

Ziaco, E., Biondi, F., Rossi, S. & Deslauriers, A. (2014) Climatic influences on wood anatomy and tree-ring features of Great Basin conifers at a new mountain observatory. *Applications in Plant Science,* **2,** apps.1400054.

Appendix A. Supporting Information

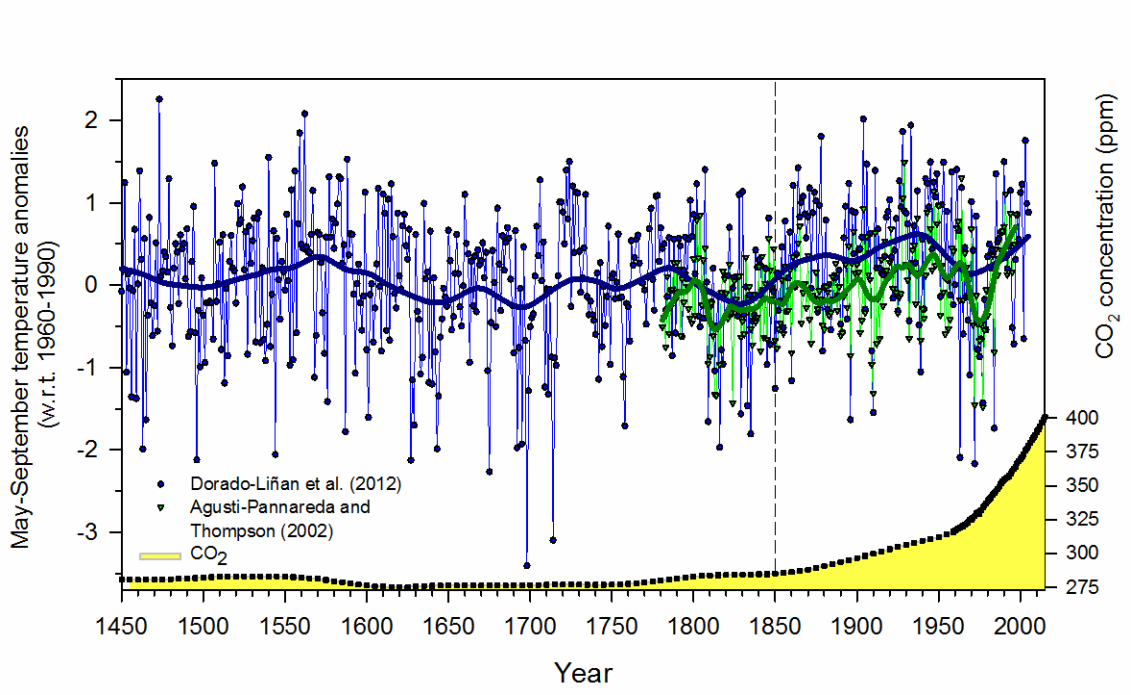

Fig. S1 Reconstructed temperature anomalies (with respect to the 1960-1990 mean) in the Spanish Pyrenees and estimated trends in atmospheric CO_2 concentrations (yellow area, right y axis). Temperature anomalies are based on Dorado-Liñan et al 2012 (blue dots) and Agusti-Pannareda and Thompson 2002 (green triangles) reconstructions. The dashed vertical line indicates the beginning of the industrial period.

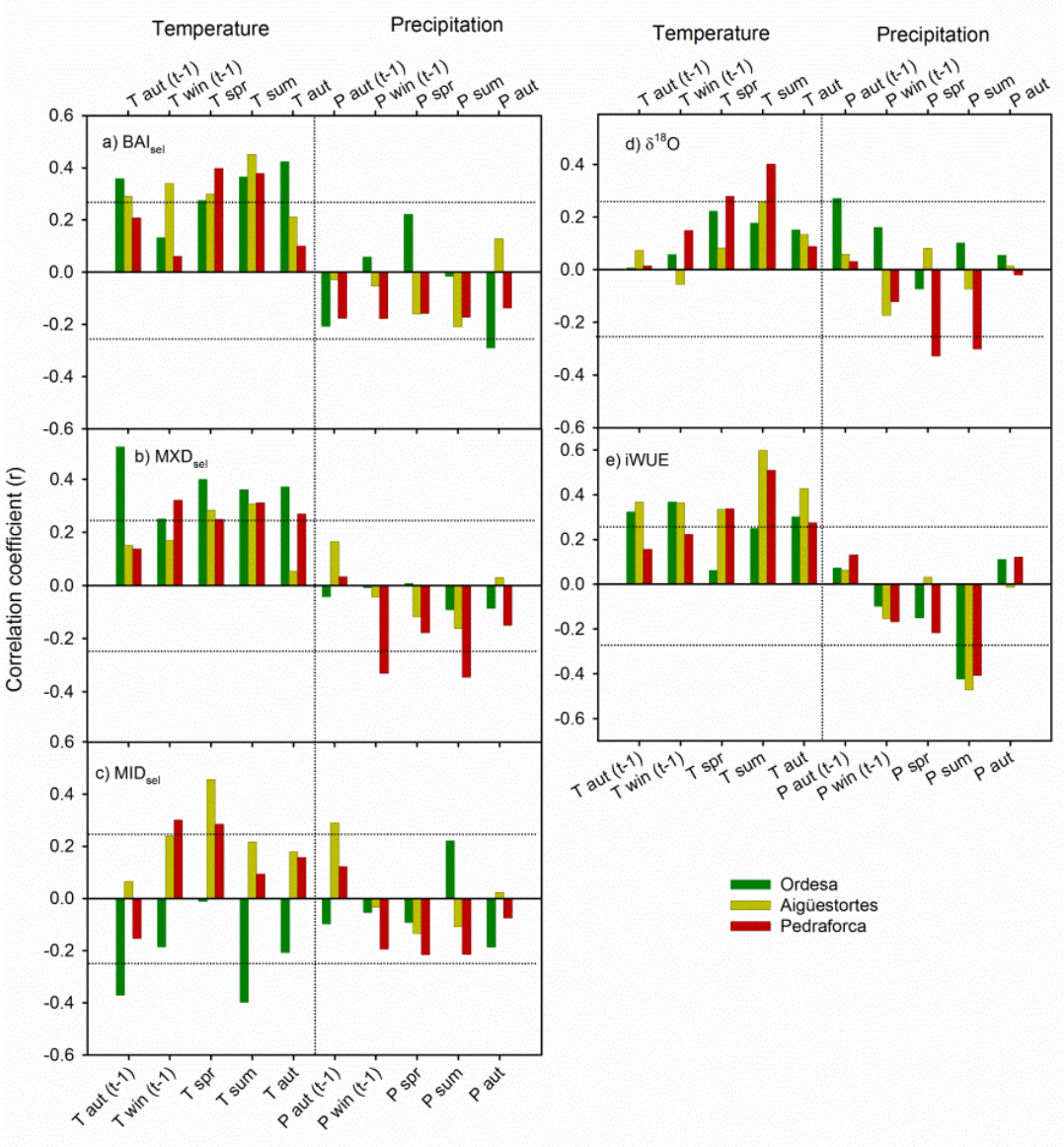

882

883 **Fig. S2** Correlation coefficients calculated between basal-area increment (BAI), maximum
884 (MXD) and minimum (MID) wood densities, oxygen isotope ratios ($\delta^{18}O$) and intrinsic water-
885 use efficiency (iWUE) with seasonal climate variables for the 1950-2008 period at the three
886 study sites (Ordesa, Aigüestortes and Pedraforca). Horizontal dotted lines indicate significance
887 levels ($P = 0.05$). Climatic variables' abbreviations are: T, temperature and P, precipitation.
888 Variables of the year prior to tree-ring formation are indicated with *t-1* and separated with a
889 vertical dotted line. Seasons are abbreviated as: aut, autumn (SON); win, winter (DJF); spr,
890 spring (MAM); sum, summer (JJA).

891

892 **Table S1** Summary of the characteristics of old trees selected at each site.

Site	Tree	DBH (cm)	Height (m)	Altitude (m a.s.l.)	Age (years)
Ordesa (ORD)	SC03	56.2	9.5	2081	637
	SC07	103.6	8	2110	654
	SC09	55.0	9.5	2247	659
	SC11	51.0	10.5	2042	412
Aigüestortes (AIG)	NE21	77.0	7	2355	731
	GE11	42.8	9	2268	603
	GE16	64.5	7.5	2275	635
	GE25	52.0	6	2273	633
Pedraforca (PED)	UP03	61.5	7.9	2196	455
	UP04	64.3	6.5	2200	644
	UP05	58.3	7.5	2229	516
	UP09	50.6	10.8	2196	500

893

894 **Table S2** Correlations calculated for all trees and the selected trees for each variable considering
895 the whole study period. Variables' abbreviations are: BAI, basal area increment; MXD,
896 maximum wood density; MID; minimum wood density. Asterisks denote significant correlations
897 ($P < 0.0001$). Sites are abbreviated as in Table S1.

Site	BAI selected vs all	MXD selected vs all	MID selected vs all
ORD	0.62*	0.82*	0.93*
AIG	0.77*	0.94*	0.86*
PED	0.96*	0.83*	0.58*

898